Metal-saturated sulfide assemblages in NWA 2737: Evidence for impact-related sulfur devolatilization in Martian meteorites

Jean-Pierre Lorand, Jean-Alix J-A Barrat, Vincent Chevrier, Violaine Sautter, Sylvain Pont

Metal-saturated sulfide assemblages in NWA 2737: Evidence for impact-related sulfur devolatilization in Martian meteorites

Jean-Pierre LORAND[1*], Jean-Alix BARRAT[2], Vincent CHEVRIER[3], Violaine SAUTTER[4], and Sylvain PONT[4]

[1]Laboratoire de Planétologie et Géodynamique de Nantes, Université de Nantes and Centre National de la Recherche Scientifique (UMR 6112), 2 Rue La Houssinière, BP 92208, 44322 Nantes, Cédex 3, France
[2]Université de Bretagne Occidentale, Institut Universitaire Européen de la Mer, Place Nicolas Copernic, 29280 Plouzané Cedex, France
[3]W.M. Keck Laboratory for Space and Planetary Simulation, Arkansas Center for Space and Planetary Science, MUSE 202, University of Arkansas, Fayetteville, Arkansas 72701, USA
[4]Muséum National d'Histoire Naturelle, Laboratoire de Minéralogie et Cosmochimie, CNRS UMR 7202, 61 Rue Buffon, 75005, Paris, France
[*]Corresponding author. E-mail: jean-pierre.lorand@univ-nantes.fr

Abstract–NWA 2737, a Martian meteorite from the Chassignite subclass, contains minute amounts (0.010 ± 0.005 vol%) of metal-saturated Fe-Ni sulfides. These latter bear evidence of the strong shock effects documented by abundant Fe nanoparticles and planar defects in Northwest Africa (NWA) 2737 olivine. A Ni-poor troilite ($Fe/S = 1.0 \pm 0.01$), sometimes Cr-bearing (up to 1 wt%), coexists with micrometer-sized taenite/tetrataenite-type native Ni-Fe alloys ($Ni/Fe = 1$) and Fe-Os-Ir-(Ru) alloys a few hundreds of nanometers across. The troilite has exsolved flame-like pentlandite ($Fe/Fe + Ni = 0.5$–0.6). Chalcopyrite is almost lacking, and no pyrite has been found. As a hot desert find, NWA 2737 shows astonishingly fresh sulfides. The composition of troilite coexisting with Ni-Fe alloys is completely at odds with Chassigny and Nahkla sulfides (pyrite + metal-deficient monoclinic-type pyrrhotite). It indicates strongly reducing crystallization conditions (close to IW), several log units below the fO_2 conditions inferred from chromites compositions and accepted for Chassignites (FMQ-1 log unit). It is proposed that reduction in sulfides into base and precious metal alloys is operated via sulfur degassing, which is supported by the highly resorbed and denticulated shape of sulfide blebs and their spongy textures. Shock-related S degassing may be responsible for considerable damages in magmatic sulfide structures and sulfide assemblages, with concomitant loss of magnetic properties as documented in some other Martian meteorites.

INTRODUCTION

Troilite, taenite, and Os-Ir alloys are essential minerals in chondritic meteorites that have escaped a high degree of hydrothermal alteration on their parent bodies (e.g., Brearley and Jones 1997). By contrast, base metal alloys or precious metal alloys have never been described in Martian meteorites. Due to magmatic redox conditions (ranging from IW to FMQ; McSween [2002] and references therein), base metal sulfides (i.e., Cu-Fe-Ni sulfides) exist in a more oxidized assemblage of metal-deficient pyrrhotite-like phases (occasionally troilite), pentlandite, chalcopyrite, and secondary pyrite. In spite of being accessory minerals (0.01–0.5 wt%), sulfides are important petrogenetic minerals for SNC meteorites, tracing redox conditions (Lorand et al. 2005; Chevrier et al. 2011) and carrying rock magnetic susceptibility (Rochette et al. 2001, 2005). Monoclinic pyrrhotite is an important ferromagnetic mineral and a significant contributor to the remnant magnetic field in the upper (30 km) crust (Louzada et al. 2011). Through sulfur isotopic compositions and sulfate/sulfide ratios, sulfides

have proven to be reliable indicators of Martian hydrothermalism (Burgess et al. 1989; Greenwood et al. 2000; Farquhar et al. 2007).

It is widely assumed that the Martian crust in the area of impact craters may have been demagnetized by shock impacts that heated rocks above the Curie temperature of pyrrhotite (320 °C) (Rochette et al. 2005; Louzada et al. 2011). TEM studies of troilites in shocked meteorites show spark-shaped grains, accumulated quenching-induced substructures, and defects/hardening (Joreau et al. 1996). Pressure twins have been described in Shergotty pyrrhotite (Stöffler et al. 1986). As a volatile element, sulfur is thought to be volatilized during impact events, perhaps contributing to sulfate production on Mars (Knauth et al. 2005). Malavergne et al. (2001) described S-bearing clinopyroxene melt pockets in very localized areas of shergottites (Shergotty, Zagami), as well as in Nahkla and Chassigny. Here, we described a unique metal-rich mineral assemblage in the recently characterized Chassignite Northwest Africa (NWA) 2737 that provides strong evidence for impact-related S devolatilization on Mars. This assemblage is a product of the shock event this meteorite underwent within the Martian crust.

MAIN PETROGRAPHIC FEATURES OF CHASSIGNITES

The Chassignite subclass, now represented by two meteorites described so far, is dunites with cumulate textures derived from the shallow-level Martian crust (McSween and Treiman 1997; McSween 2002). They both have the same crystallization age (1.3–1.4 Ga) and cosmic-ray exposure age of 11 Ma (Nyquist et al. 2001) which suggest ejection from the same site on Mars during a single impact event.

NWA 2737 is a 611 g dunite showing closely similar petrological features to Chassigny meteorite and significant differences as well (Beck et al. 2006). It shows a cumulate texture of millimeter-sized olivine (89 wt%); mostly anhedral dark (?) crystals of rather homogeneous composition (Fo78 ± 0.5 wt%); and chromite occurring mainly as idiomorphic crystals inside olivine and as intercumulus, anhedral grains. Chromite compositions show core-rim evolution from $Cr_{83}Usp_{3.6}Sp_{13}$ to $Cr_{13}Usp_{66}Sp_{21}$ corresponding to Al-Fe^{3+}-Ti enrichment trend. Intercumulus minerals are augite (3.1 wt%), low-Ca pyroxene (opx-pigeonite), analbite glass (1.6 wt%; vitrified by shock), and apatite (0.2 wt%). Like the olivine in Chassigny meteorite, large magmatic inclusions, up to 150 μm in diameter, are present in NWA 2737 olivine; euhedral daughter minerals are chromite, augite/pigeonite, olivine, and kaersutitic amphibole set up in a K-Si-Al-rich glass. Another accessory mineral is baddeleyite, detected during this study (two-phase grain in association with apatite or Fe-Ti oxides, whether ilmenite or pseudobrookite). White fracture planes are filled with Ca-carbonates (of uncertain origin, see below). Although a hot desert find, NWA 2737 escaped strong desert weathering and displays low Ba and Sr contents (a few baryte veinlets were observed in the studied thin section with the SEM). Chassigny meteorite shows Ca-sulfide veins (gypsum or bassanite) of presumably Martian origin postdating igneous minerals (Wenworth and Goodings 1994); no such mineral has been identified with the SEM in our thin section of NWA 2737.

The most striking differences between NWA 2737 and Chassigny is the large number of metallic Fe particles in planar defects that give the dark color to NWA 2737 olivine (Pieters et al. 2008). These shock features, related to ejection from Mars, have been studied in detail by Van de Moortèle et al. (2007), Treiman et al. (2007), Bodgard and Garrison (2008), and Bläss et al. (2010) who reached somewhat different conclusions regarding the number of shock events (one or two), shock temperatures, and the origin of metallic iron. Bodgard and Garrison (2008) suggested a two-stage shock event, one, the most severe (S5–S6 in the Stöffler et al. [1991] nomenclature corresponding to shock pressure of 45–55 Gpa), heated NWA 2737 to 300–500 °C (perhaps 800 °C) and buried it in an ejecta blanket to a depth of 1–20 m. The second shock event, 11 Ma ago, heated NWA 2737 to not more than 400 °C and ejected it from Mars. Regardless of their age, both impact events have triggered degassing but no partial melting. However, according to Bläss et al. (2010), nanometric iron particles were not formed by in situ reduction but result from disproportionation reactions of divalent iron in the olivine lattice; polygonized dislocation cores incorporated trivalent iron, leaving 0 valence state Fe as nanometric particulates.

ANALYZED SAMPLES AND ANALYTICAL METHODS

Accessory sulfides were studied on one polished thick section of approximately 1×0.5 cm using the same method as in Lorand et al. (2005) for Shergottite sulfides and Chevrier et al. (2011) for Nahklite sulfides. Sulfide grains were located by systematic traversing in reflected light microscopy at magnifications ×20 to ×1000. A scanning electron microscope (TESCAN VEGA II, MNHN, Paris) operating at 20 kV in the high vacuum mode, was used to detect and identify metal micronuggets in base metal sulfides. Another set of semi-quantitative analyses of base metal sulfides and Fe-Ni alloys was done with the same apparatus at 15 kV using an EDS detector.

Electron microprobe analyses were done with a CAMECA SX 50 electron microprobe (CAMPARIS, Paris) operating at 15 kV accelerating voltage, 10 s/peak

Table 1. Accuracy of electron microprobe analyses of base metal sulfides

Troilite (Del Norte County, California)*	Chevrier et al. (2011) ($n = 36$)	This study ($n = 10$)
wt%		
Fe	63.43 ± 0.23	63.30 ± 0.30
Ni	nd	0.03 ± 0.01
Co	nd	
Cu	nd	
Zn	nd	
S	36.56 ± 0.20	36.31 ± 0.2
O	< 0.1	
Total	99.99	99.64
S (atom%)	49.98 ± 0.1	50.0 ± 0.1
Atom metal (on 1 atom S)	0.997	1.000 ± 0.006

and 10 s/background counting times and a sample beam of 40 nA. Cobalt and Cu were measured with pure metal standards, Fe and S with pyrite (FeS_2), Ni with synthetic oxide (NiO), Zn with sphalerite (ZnS), oxygen with hematite (Fe_2O_3), and silica with wollastonite ($CaSiO_3$). Silica and oxygen were added to the analytical routine to check any possible contaminations of the sulfide analyses by surrounding silicates. Accuracy of EMP analyses was checked by repeated analysis of Del Norte County natural troilite (stoichiometric FeS), a well-known terrestrial troilite occurrence previously studied by X-ray diffraction (Carpenter and Bailey 1973). This external standard was analyzed every 10–15 analyses to evaluate potential drifts on metal-to-sulfur ratios. Our mean value, based on 10 spot analyses, indicate stoichiometric Fe/S atomic ratios (1.00 ± 0.01), in excellent agreement with previously published analyses (Table 1).

SULFIDE MINERALOGY AND NATIVE METAL ASSEMBLAGES

Sulfide modal abundance was estimated by image analysis, following the method outlined in Lorand et al. (2005) and Chevrier et al. (2011). NWA 2737 is sulfide poor (0.01 ± 0.005 wt%), the modal sulfide abundance in NWA 2737 is about half that of the Nakhlites (Chevrier et al. 2011), and depleted by a factor of 10–50× compared with shergottites (e.g., Lorand et al. 2005). Sulfides are not detected in the mass balance calculation of the whole-rock Ni budget. Fe-Ni sulfides are homogeneously distributed throughout the polished thin section of NWA 2737, mostly as intergranular blebs inside olivine grain boundaries, at the contact between chromite and olivine, olivine and pyroxenes, or chromite and glassy analbite pockets (Fig. 1). No solitary sulfide inclusion has been observed inside olivine and chromite,
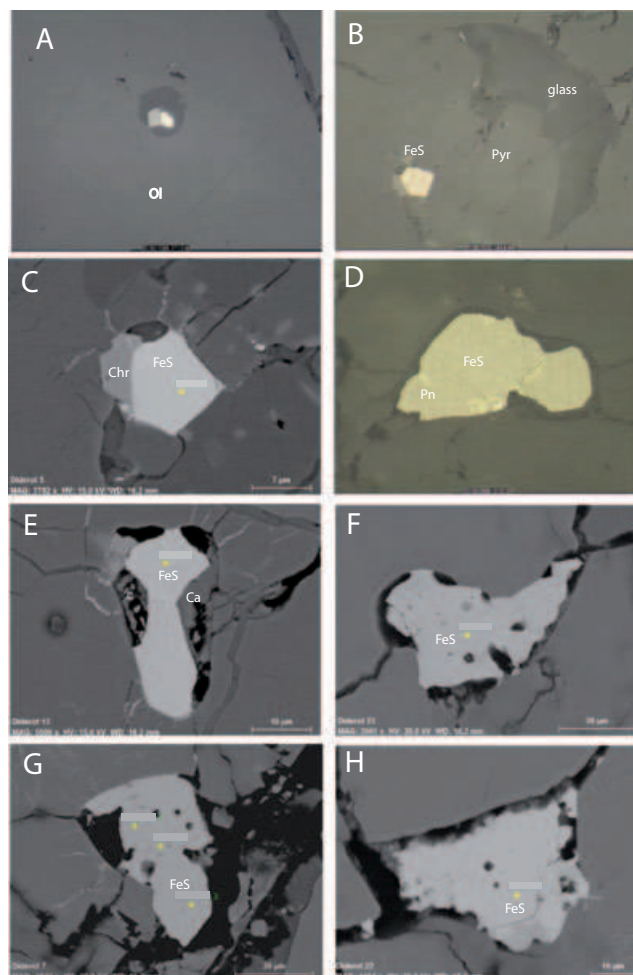

Fig. 1. Microphotographs of sulfides in NWA 2737 (A, B, D: plane-polarized reflected light microscope; C, E, F, G, H: Scanning electron microscope photographs in BSE mode): A) Olivine-hosted porphyritic inclusion showing troilite (light gray) associated with chromite (medium gray) inside glass. B) Larger inclusion composed of euhedral pyroxene crystals (Pyr), troilite (FeS), chromite (medium-gray), and glass. C) Enlargement of B (chr: chromite crystal), note the small shock-related decompression cracks filled with iron (oxy)hydroxide of likely terrestrial origin. D) Partly resorbed interstitial troilite coated with Ca carbonate (Ca); note the pentlandite flames (Pn) and films inside the troilite. E) Highly resorbed intergranular troilite; note the large amount of Ca carbonate inside the cavity. F–H) Several examples of spongy intergranular troilite. Note how etched and denticulated the troilite appears as a result of impact shock.

nor in pyroxenes; by contrast, the large, porphyritic magmatic inclusions in olivine always show a tiny sulfide bleb, less than 5×3 μm in maximum dimension, always pasted on chromite. The sulfide may be molded (reshaped) in between daughter crystals of olivine and pyroxenes (Figs. 1A–C).

Intergranular sulfides are anhedral bodies ranging between 3 and 60 μm in maximum dimension. No

preferential association with chromite is observed. However, the three largest blebs (up to 60×40 μm) occur in contact with chromite. These are elongated blebs showing contorted or highly denticulated rims. Other intergranular sulfides display various shapes, from triangular in outline, when sited at triple junctions of olivine crystals, to ovoid grains. Actually most intergranular sulfides display textural evidence of incipient resorbtion, such as highly denticulated rims, embayments, vugs, and bubbled textures (Figs. 1F and 1G). The SEM study shows that vugs and bubbles are empty. By contrast, many intergranular sulfides are embedded in calcite veins which may totally enclose the sulfides (Figs. 1D and 1E). Details of sulfides-calcite textural relationships clearly show that calcite has filled the spaces previously occupied by sulfide blebs, as well as the vugs and embayments inside the sulfides. Some sulfide blebs look like skeletal remnants totally invaded by calcite.

Whether enclosed in magmatic porphyritic inclusions or intergranular, sulfides consist in a pyrrhotite-like phase, by far predominant over the other sulfides identified with the optical microscope. The pyrrhotite was identified as troilite (FeS) with the SEM and EMPA (see below); thus it will be referred to as troilite. The largest troilite grains are polycrystalline aggregates, showing granoblastic texture with subgrain boundaries meeting at 120°. The largest blebs show fracture planes (broken into two or three pieces or unequal size), which served as the nucleus for pentlandite flames and pathways for terrestrial alteration. However, the latter alteration is not widespread; only the most fractured grains exhibit incipient alteration into Fe oxi-hydroxide network inside the pyrrhotite (Fig 2E). Pentlandite is the second most common sulfide in NWA 2737, although it always occurs in very low modal proportions, representing less than a few percent by volume of the BMS grains. Denticulated flames intergrown with troilite, less than 5 μm across, are preferentially located along fracture planes and over troilite rims (Fig. 1D); massive shaped grains are lacking. No chalcopyrite, or pyrite has been observed.

Fe-Ni alloys are tiny grains, up to 5×3 μm in maximum dimension, sometimes euhedrally shaped, very bright in reflected light microscopy. Four of the five Fe-Ni alloy grains detected in our NWA 2737 polished thin section occupy the rim of host pyrrhotite while being part of the Fe-Ni sulfide grain (Figs. 2A, 2B, and 3A); some develop euhedral grain boundaries. One Fe-Ni alloy grain is included in the troilite (random sectioning effect?). Fe-Ni alloys are clearly overgrown by poikilitic pentlandite flames that show up inward development inside troilite grains. Os-Ir alloys have been identified during the SEM investigation operating in the BSE mode. These are two minute anhedral grains, one 0.8 μm across and the other approximately 1 μm. Unlike Fe-Ni
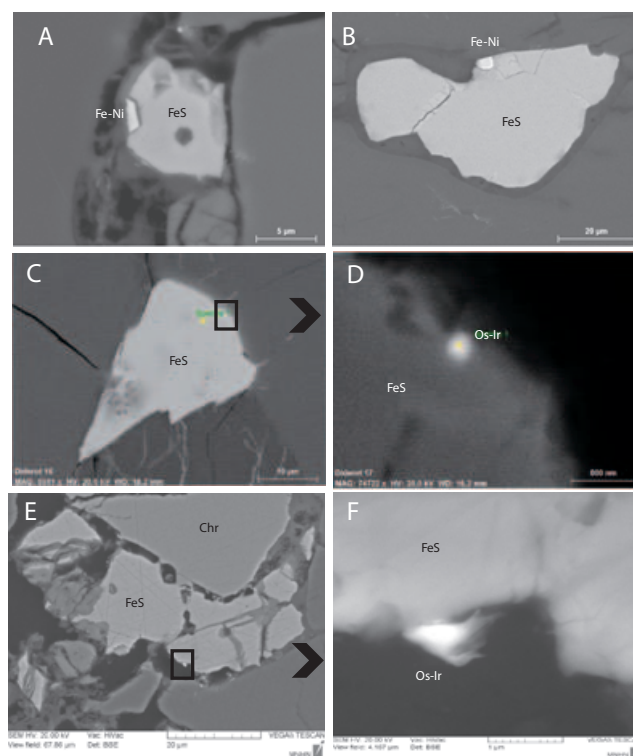

Fig. 2. BSE images of Ni-Fe alloy and Os-Ir alloys in NWA 2737. A) External granule of Fe-Ni alloy associated with a troilite droplet inside intergranular space between olivine grains. B) External granule of Fe-Ni alloy associated with a large, homogeneous troilite (FeS). Note that both alloys are clearly part of the sulfide grain. C, D) External granule of submicrometric Os-Ir alloy pasted on a troilite at triple junction between olivine (medium-gray) and pyroxene (dark-gray; image D is an enlargement of image C). E and F) External granule of Os-Ir alloy associated with a partly oxidized pyrrhotite grain showing development of iron (oxy)hydroxides along fracture and cleavage plans; chr = chromite. Note the marginal position and the irregular shape of the alloy with respect to troilite.

alloys, both Os-Ir alloys are pasted on the rim of highly resorbed troilite grains, not part of the grain (Figs. 2D and 2F). The EDS spectra identified Fe, Os, and Ir as major elements, Ru as minor element (Fig. 3B) but no other platinum group metal was detected. However, the exact amount of Fe actually present in the two Os-Ir alloys cannot be determined as the analysis is strongly biased by neighboring troilite. No Fe-Ni sulfide bleb shows Fe-Os-Ir and Fe-Ni alloys to coexist in a single grain.

MINERAL CHEMISTRY

Troilite shows a highly uniform total metal-to-sulfur ratio (M∕S) of 1.019 ± 0.009 (30 spot analyses on 14 grains; Fig. 4). As shown by the analyses of Del
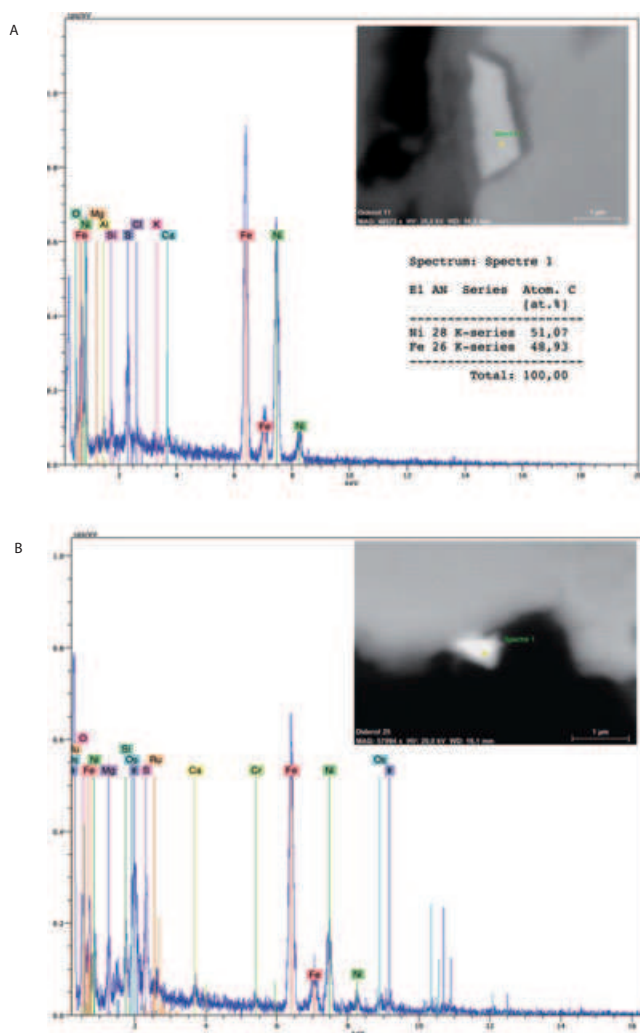
Fig. 3. EDS spectra of Fe-Ni alloy (A) and Os-Ir alloy (B). The S peaks in both diagrams can be attributed to excitation of associated troilite under the electron beam; note the intensity of the Fe and Ni peaks in diagram B, which is too high to be solely attributed to contamination by the sulfide.

Fig. 4. Frequency diagram of the compositions of troilite in NWA 2737 compared with nahklite pyrrhotite compositions (Chevrier et al. 2011). *n* represents the number of electron microprobe analyses.

Norte County troillite, done with the same analytical conditions as for NWA 2737, the slight metal excess in NWA 2737 troilite does not result from analytical bias; it is more likely due to slight metal-oversaturation. The results of EMP analyses and semi-quantitative EDS analyses agree fairly well at 1 sigma level (1.019 ± 0.01 versus 0.99 ± 0.01; Table 2), bearing in mind that EDS analyses do not take into account minor elements that may amount up to approximately 1 wt% (Table 1). There is no difference between enclosed pyrrhotite in porphyritic magmatic inclusions and intergranular grains. Both are weakly nickeliferous (Ni < 1.05 wt%) troilite. Random variations in the Ni content can be observed inside a single troilite grain (0.2–1 wt% Ni), irrespective of M/S or alloy occurrences. Such patchy
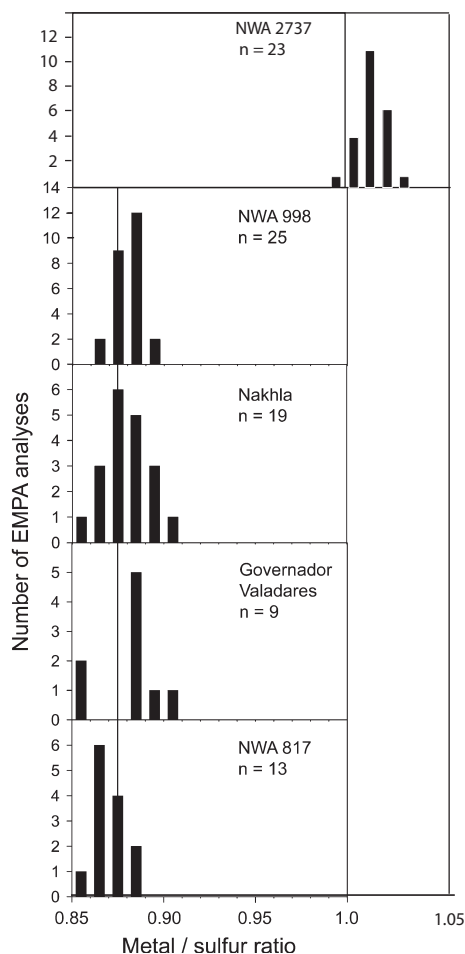
variations are not due to beam overlap on pentlandite flames that would cause M/S to increase (e.g., Lorand et al. 2005). The five troilites coexisting with Fe-Ni alloys show similar Ni concentration ranges as the metal-free grains (Table 1). Chromium is a minor element of NWA 2737 troilite (0.02–0.11 wt%) regardless of whether the analyzed BMS is close to chromite or not. However, the three grains adjacent to chromite are more Cr-rich (up to 0.8 wt% Cr). Their elevated Cr contents cannot be analytical artifacts because they were observed with both the EMP and the SEM over a distance > 10 μm from the chromite.

The small, highly denticulated pentlandite flames inside troilite were not suitable for EMP analyses. Semi-quantitative EDS analyses indicate Fe/Ni atomic ratios > 1 (1.2–1.9), as usual for such pentlandite occurrences coexisting with troilite (e.g., Misra and Fleet 1973; Lorand 1985; Etschmann et al. 2004).

Table 2. Representative electron microprobe analyses of NWA 2737 base metal sulfides.

wt%	Tr	Tr	Tr	Tr	Tr	Tr	Tr	Tr	Tr
Fe	63.39	62.28	63.73	63.46	62.51	63.83	63.41	63.44	62.77
Ni	0.93	0.21	0.10	0.56	1.03	0.77	0.41	0.24	0.38
Co	nd	nd	nd	nd	0.28	0.23	0.33	0.07	0.21
Cu	nd	nd	nd	nd	nd	nd	nd	nd	nd
Cr	0.03	0.06	0.03	0.06	nd	0.02	0.38		0.54
Mn	0.01	0.02	nd	0.03	nd	nd	nd	0.07	0.04
Zn	nd	nd	0.08	nd	nd	nd	nd	0.05	0.03
O	0.05	0.08	0.18	nd	nd	0.08	0.15	0.09	0.05
S	36.30	36.40	36.32	36.39	36.45	36.81	36.46	36.12	36.27
Total	100.71	99.05	100.44	100.50	100.25	101.74	101.14	100.577	100.27
M/S	1.019	0.99	1.013	1.014	1.00	1.014	1.019	1.025	1.015
wt%	Tr	Tr	Tr	Tr	Tr	Tr	Tr	Tr	Tr
Fe	62.63	63.23	63.77	62.84	63.19	63.63	63.79	63.38	62.65
Ni	0.46	0.42	0.28	0.11	0.20	0.21	0.61	0.33	0.89
Co	0.43	0.18	nd	nd	nd	nd	nd	nd	nd
Cu	nd	nd	0.02	nd	nd	nd	nd	nd	nd
Cr	0.84	0.89	0.11	0.04	0.04	0.06	0.04	0.028	0.05
Mn	0.05	0.07	0.01	0.05	0	0.04	0.01	0	0.02
Zn	nd	nd	nd	0.14	nd	nd	nd	nd	nd
O	0.07	0.14	0.09	0.18	0.14	0.18	0.30	0.34	0.38
S	36.40	36.25	36.29	36.02	36.00	36.09	36.11	36.16	36.38
Total	100.91	101.18	100.57	99.38	99.57	100.22	100.72	100.24	100.37
M/S	1.019	1.029	1.018	1.00	1.015	1.02	1.028	1.015	1.00
at %	Pn	Pn*	Pn*	Pn*	Pn*	Fe-Ni* alloy	Fe-Ni* alloy		
Fe	40.75	29.68	31.5	31.46	34.83	49	48.5		
Ni	24.97	22.85	19.9	20.44	16.7	51	51.5		
Co	0.46	nd	nd	nd	nd	nd	nd		
Cu	0.95	nd	nd	nd	nd	nd	nd		
Cr	0.04	nd	nd	nd	nd	nd	nd		
Mn	0.05	nd	nd	nd	nd	n.d	nd		
Zn	nd	nd	nd	nd	nd	nd	nd		
O	nd	nd	nd	nd	nd	nd	nd		
S	32.73	47.47	48.65	48.1	47.47	nd	nd		

Tr = troilite; Pn = pentlandite; *EDX semi-quantitative analyses (at %).

The two Fe-Ni alloys analyzed with the SEM (Fig. 3) have taenite-tetrataenite composition, close to $Fe_{0.51}Ni_{0.49}$. The nanometric metal particles inside olivine are more Fe-rich ($Fe_{0.97}Ni_{0.07}$ to $Fe_{0.66}Ni_{0.34}$; Van de Moortèle et al. 2007).

DISCUSSION

The occurrence of Fe-Ni metals in Fe sulfides is consistent with the large number of metallic Fe particles in planar defects that give the black color of NWA 2737 olivine (Beck et al. 2006). Metal phases in NWA 2737 are obvious products from the reduction reactions that took place during shock events; however, the mechanisms in silicates and sulfides were probably different.

Opaque trace phases in NWA 2737 markedly differ from what is currently reported in Martian meteorites, i.e., metal-deficient pyrrhotite ($Fe_{1-x}S$; $0.05 < x < 0.13$) associated with trace amounts of pentlandite, Cu-sulfides (chalcopyrite, cubanite) and iron disulfides (pyrite or marcasite; Lorand et al. 2005; Chevrier et al. 2011). Pyrite or marcasite is especially abundant in the Chassigny meteorite where single-phase pyrite blebs were reported (e.g., Floran et al. 1978; Rochette et al. 2001; Greenwood et al. 2000) in addition to metal-deficient pyrrhotites (Lorand, and Chevrier, in prep.). By contrast, no pyrite has been identified in NWA 2737.

Os-Ir alloys, Fe-Ni alloys, and troilitic pyrrhotites are essential minerals in carbonaceous chondrites (e.g., Brearley and Jones 1997; Kimura et al. 2011); however, these minerals occupy very distinct textural sites compared with NWA 2737, namely as complex refractory metal nuggets (RMN = Os-Ir-Ru-Rh-Pt-Re-Mo) enclosed in calcium-aluminum-rich inclusions for Os-Ir alloys, Fe-Ni

metals of various origin (condensation, reduction of ferro-magnesian silicates, inside and outside chondrules or late-metamorphic minerals) and matrix component for the troilite, mostly replaced by poorly characterized sulfide phases during aqueous alterations on parent bodies. Ni metal particles in carbonaceous chondrites have various origins, including secondary product of heating in the parent body after aqueous alteration (Kimura et al. 2008) or pentlandite alteration product after impact-induced heating (e.g., Kimura and Ikeda 1992). In NWA 2737, both metal phases (i.e., taenite or tetrataenite and Fe-Os-Ir alloys) occur inside troilite and their origin is closely related to this sulfide. No replacive relationship between pentlandite and Fe-Ni metals has been observed.

Evidence of Sulfur Devolatilization Affecting Magmatic Sulfides in NWA 2737

Two lines of evidence support a magmatic origin for NWA 2737 sulfides: (1) their shape of immiscible sulfide melts—from nearly spherical droplets to polyhedral grains with convex-inward margins, (2) their pyrrhotite-rich assemblages. As documented in other Martian meteorites, sulfide liquid separated at a late-magmatic stage as suggested by (1) the overabundant intergranular sulfide blebs at boundaries between augite and olivine and sulfide pocket at triple junction of olivine crystals (now sealed by Ca carbonates), (2) the lack of solitary sulfide inclusions in cumulus silicates (olivine, chromite), (3) NWA 2737 troilite shows quite homogeneous but low Ni contents (1.0 ± 0.5) suggesting equilibration with evolved silicate melts.

It has long been shown that pyrrhotite Fe/S ratios correlate negatively with oxygen fugacity if sulfides occur as accessory minerals, acting as passive indicator of redox conditions (Barton 1970; Eggler and Lorand 1993; Lorand et al. 2005). Nonstoichiometry in pyrrhotites is caused by incorporation of trivalent iron that generates vacancies and decreases the M/S ratio (Vaughan and Craig 1978). Thus, the uniformly high (stoichiometric) M/S ratio of NWA 2737 pyrrhotites is at odds with the oxidizing crystallization conditions that are postulated for Chassigny (FMQ-1 log unit; Delaney and Dyar 2001; Treiman et al. 2007). Based on change in the vanadium valence with oxygen fugacity, Beck et al. (2006) even estimated a higher magmatic fO_2 in NWA 2737 than in Chassigny meteorite (FMQ + 0.3 log unit). As shown by the log f_{S_2}-T diagram of Fig. 5, the FMQ-pyrrhotite buffer (FMQ-Po) imposes pyrrhotite compositions with M/S ≤ 0.9 (as observed for instance in nahklites, Chevrier et al. 2011) eventually crystallizing pyrite on cooling below 200 °C. By contrast, troilite can coexist stably with Fe-Ni alloys over a very narrow window close to the Fe-FeS curve, well below the conditions defined by FMQ-Po. By reducing oxygen
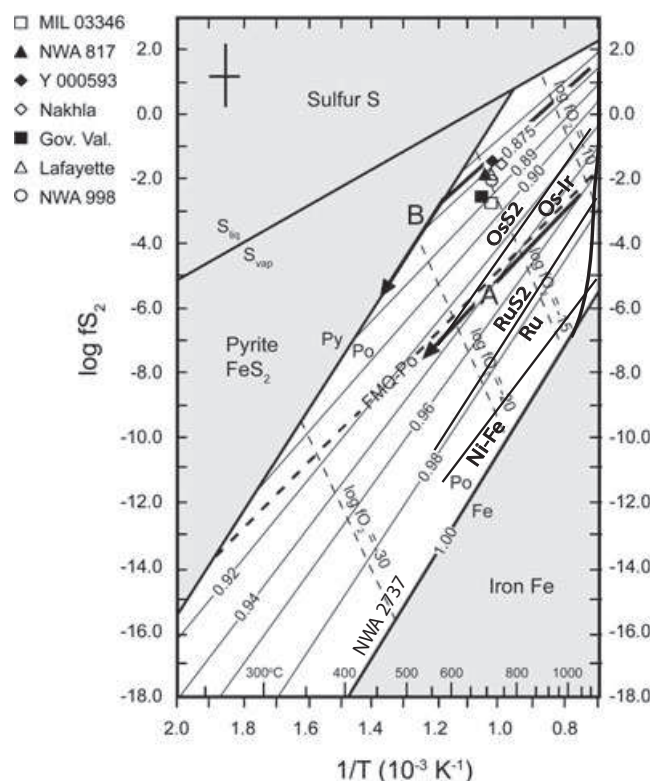

Fig. 5. Log fS_2 versus 1000/T diagram showing equilibrium compositions of troïlite in NWA 2737 compared with nahklites and Chassigny (after Lorand et al. 2005; Chevrier et al. 2011). Pyrrhotite Fe atomic isopleths from Toulmin and Barton (1964) were converted into metal-to-sulfur ratios for clarity. Dashed curves labeled with oxygen fugacity are for the reaction: $3FeS + 2O_2 <=> Fe_3O_4 + 3/2S_2$ (pyrrhotite-magnetite equilibrium). FMQ-Po buffer from Eggler and Lorand (1993). Sulfidation curves for Ni-Fe alloys from Vaughan and Craig (1978), Barin (1995), and Bockrath et al. (2004) for Os, Ir, and Ru, respectively. Note that troilite cannot coexist with Ru-poor alloys. Path A: subsolidus cooling controlled by FMQ-Po; path B: reduction path from a Chassigny-type pyrite-pyrrhotite assemblage.

fugacity via volatilization of oxygen, shock processes in NWA 2737 may have contributed to reduction of metal-deficient pyrrhotite compositions into troilite, while destroying the pyrite-like phases.

Decreasing oxygen fugacity at the whole-rock scale may account for the very homogeneous troilite compositions analyzed within prophyritic inclusions that are expected to have been closed systems during the shock event(s). However, this decrease was coeval with shock-induced sulfur vaporization. Compared with the regularly faceted enclosed sulfides, sulfide blebs that occur interstitially with the main silicates display highly denticulated shapes showing signs of volume loss (now filled up with Ca-carbonates). Their spongy textures may result from bubbling of S vapor. Fe-Ni alloys formed in situ, by volume diffusion of Ni-Fe, where S preferentially

escaped. This is the reason why NWA 2737 Ni-Fe alloys are tiny grains, sometimes enclosed, sometimes marginal with respect to troilite, never forming rims around troilite as commonly reported for Ni_3Fe awaruite-replacing BMS phases in serpentinized terrestrial peridotites that experienced low-temperature (<200 °C) desulfurization reactions (e.g., Lorand 1985). The highly heterogeneous distribution of metals between troilite blebs is a straightforward consequence of devolatilization which is by definition a very heterogeneous process depending on the diffusion rate of S through the pyrrhotite lattice, pressure twins, defects, temperature, pressure, etc.

There are several lines of evidence suggesting that sulfur may have started to escape at high temperature, consistent with the temperature range postulated for the first shock event (400–500 °C). Copper seems to have been vaporized from BMS grains, resulting in very low Cu content (no Cu sulfide and scarcely detected Cu concentrations in troilite). The total removal of pyrite from NWA2737 can be related to its incongruent melting to pyrrhotite + sulfur that occurs above 740 °C at P = 1 bar (Kullerud et al. 1969). Shock-related heating to this temperature should have also resulted in the breakdown of any pre-existing pentlandite which decomposes above 610 °C (Kullerud et al. 1969). Kimura et al. (2011) recently suggested that tiny Ni-rich (51–69 wt% Ni) Fe-Ni-Co metal phases associated with troilite in some CM chondrites are pentlandite decomposition product formed by impact-induced heating. Ordered tetrataenite (gamma ordered fcc, equiatomic FeNi) is stable below 320 °C covering a very narrow compositional range (Ni/Fe = 0.5 ± 0.02); however, it undergoes phase transformation above 320 °C (Yang et al. 1997). In ordinary chondritic meteorites, tetrataenite formed from homogeneous low-Ni paramagnetic fcc taenite phase by metamorphism and very slow cooling (1–100 °C Myr^{-1}, Clarke and Scott 1980), i.e., 5–7 orders of magnitude slower than that experienced by NWA2737 postshock assemblages on the parent body, giving rise to complex exsolution patterns in the metal phase (e.g., Yang et al. 1997; Uehara et al. 2011). Our SEM study did not revealed exsolution microtexture inside NWA 2737 alloy grains; the latter exsolved from the troilite, perhaps from former pentlandite.

Evaluation of crystallization temperatures for NWA Fe-Ni alloys can be only semiquantitative, as no crystallographic parameters could be obtained from such tiny grains: synthetic taenite coexisting with troilite above 400 °C display less than approximately 45% Ni at 725 °C (Karup-Møller and Makovicky 1995), and no more than 30% at 900 °C, as shown by quenched immiscible sulfide blebs in highly reduced terrestrial basalts from the Disko island (Greenland) (Pedersen 1979; see also Kullerud et al. 1969). Compared with the aforementioned compositions, NWA 2737 FeNi alloys are more Ni-rich, a feature that reflects either small scale equilibrium or re-equilibration of the Fe-Ni partitioning between alloy and troilite to lower temperature. It is notable that Ni, a minor element in the troilite diffused into the alloy creating a Ni-poor dark halo around some of the coarsest grains. Then, the Fe-Ni alloys may have served as nuclei for pentlandite growth. Newly formed pentlandite flames are shaped in a form expected from homogeneous nucleation process in the typology of pentlandite exsolution (Etschmann et al. 2004); according to that typology, NWA 2737 pentlandite typically exsolved over a temperature range of 200–300 °C. It is worth noting that the tie-lines linking NWA troilite composition with taenite in the Fe-Ni-S system are not consistent with those calculated at 25 °C (Misra and Fleet 1973), nor with mineral pairs occurring in terrestrial ultramafic rocks that display troilite + awaruite compositions (Ni_2Fe-Ni_3Fe; cf. Lorand 1985, 1988). The diffusion of Ni between troilite and taenite was blocked at higher temperature, thus leaving residual Ni in NWA troilite slightly higher than expected at 25 °C. Nickel and Fe diffuse in pyrrhotite structures at about 10^{-9} cm^2 s^{-1} at 480 °C for Fe in Po and 720 °C in NiS (Ewers 1972; MacQueen 1979). Metal ions move between hexagonal close packed S^{2-} ions due to the defective metal sublattice. In nondefective metal sublattice, diffusion coefficients are seriously decreased; likewise, shock pressure has a blocking effect on Fe-Ni diffusion by decreasing the S-S interatomic distance. Both parameters may have had blocking effects on the Ni-Fe partitioning between troilite and pentlandite and between troilite and alloys.

Furthermore, evidence of high temperature diffusion in NWA 2737 troilite is the occurrence of detectable amounts of chromium in the troilite grains in contact with chrome spinel. For the oxygen fugacity of the FMQ-Po buffer, chromium mainly occurs as trivalent chromium (Murck and Campbell 1986; Mallmann and O'Neill 2009) which preferentially partitions into octahedral sites of Cr-spinel. Its chalcophile behavior, recorded by NWA 2737 troilite, suggests that Cr was able to entering the octahedral sites of troilite; however, trivalent Cr produces a charge excess which must be balanced by an increasing number of vacancies in the pyrrhotite sublattice as follows:

$$3M^{2+} = 2M^{3+} + \text{Vacancy} \qquad (1)$$

Reaction 1 may also accommodate lattice deformation resulting from the smallest size of trivalent chromium compared with Fe and Ni. However, no correlation between Cr contents and metal deficiency has been noted in

NWA 2737, which makes the hypothesis of divalent chromium replacing divalent Fe on a one for one basis more likely. Divalent chromium is also of interest for any discussion of redox reactions involved in NWA 2737 petrogenesis. Divalent chromium becomes abundant in reduced melts for oxygen fugacity close to the buffer iron-wustite (IW; Roeder and Reynolds 1991). Enstatite chondrites, the most reduced natural mineral assemblages known in the solar system (equilibrated at IW-5 to IW-7 log units), contain Cr-bearing troilite showing up to 3.0 wt% Cr (Ikeda et al. 1997). Thus, NWA 2737 troilite Cr-bearing compositions are consistent with the dramatic decrease in oxygen fugacity conditions resulting from impact-related devolatilization, coupled with high-temperature heating allowing Cr to diffuse from Cr-spinel to adjacent sulfides. Unfortunately, no diffusion coefficients are available for chromium in pyrrhotite structures.

Origin of Os-Ir Alloys

Like Fe-Ni alloys, the two Fe-Os-Ir alloys detected with the SEM obviously formed from the Fe-Ni sulfide assemblage; however, the fact that these alloys are systematically offset from the troilite mass raise some question about their origin: whether they formed as troilite exsolution products or from former Os-Ir-richer minerals is presently unclear, yet several lines of evidence argue for the former interpretation. Os-Ir alloys are among the most refractory metals known in the solar system, their crystallization temperature ranging between 2500 and 3060 °C (Bird and Bassett 1980). Ru-poor Os-Ir alloys have been reported along with highly reduced minerals (SiC, Fe silicide, carbides, Fe) in podiform chromitites (Bai et al. 2000); thus, their occurrence in NWA 2737 is consistent with the overall reducing process this meteorite has experienced. Both Os and Ir are strongly chalcophile and can be incorporated into the octahedral sites of pyrrhotites at wt percent concentration levels at magmatic (950 °C) temperatures (Bullanova et al. 1996; Alard et al. 2000; Lorand and Alard 2001). Trivalent Os and Ir enter the pyrrhotite if octahedral metal vacancies are abundant, thus deforming the pyrrhotite sublattice (Li et al. 1996; Barnes et al. 2001). At a given temperature, the solubility of Ir and Os in pyrrhotite falls exponentially with decreasing fS_2, reaching part-per-million concentration levels for troilite compositions (Lorand and Alard 2001; Peregoedova et al. 2004); Peregoedova et al. (2004) found Ir-rich mineral exsolution in pyrrhotite-like phase containing only 10 ppm Ir. Accordingly, by reducing the fugacity of sulfur and eliminating octahedral vacancies of pre-existing monoclinic-type pyrrhotite, the shock-induced S devolatilization may have been capable of triggering exsolution of NWA 2737 Fe-Os-Ir alloys.

Platinum-group elements are ultratrace elements in Martian meteorites, present at part-per-billion concentrations (Jones et al. [2003] and reference therein). For NWA 2737, a mass balance calculation of the Os and Ir content of BMS can be attempted by assuming similar bulk-rock Os and Ir contents in NWA 2737 and Chassigny (1.8 ppb Os and 1.2 ppb Ir; Jones et al. 2003) and both elements exclusively partitioned into the Fe-Ni sulfide phases. NWA 2737 troilite would not host more than approximately 10–20 ± 10 ppm of both Os and Ir. Taken at face values, these calculated concentrations fall within the low-T range of terrestrial metal-rich pyrrhotite measured by laser-ablation ICPMS (Lorand and Alard 2001), and consistent with experimentally determined Ir-saturation levels for troilite. Unfortunately, these solubility data cannot be refined by in situ analyses, as NWA 2737 troilite grains are too small to be analyzed with LA-ICPMS techniques. One may also surmise that Os-Ir alloys nucleated from previous pentlandite flames or because the troilite was locally Os-Ir oversaturated, due to slower diffusion rate of Os and Ir compared with the volatilization rate of S. Brenan et al. (2000) reported a self-diffusion coefficient of Os in pyrrhotite of similar order of magnitude as those of Fe and Ni that also formed alloys inside troilite. The formation of Fe-Os-Ir alloys was coeval with vaporization of host troilite that displaced the alloy grains away from the sulfide. The fact that only two Fe-Os-Ir grains were detected, both at a submicrometric scale, is consistent with a local (not widespread) nucleation mechanism. The Ru-poor compositions of the Fe-Os-Ir alloys is consistent with the higher preference of Ru for Fe-Ni sulfides (Fleet and Stone 1991; see also Li et al. 1996). As shown in Fig. 5, Os-Ir alloys can coexist with Ru-bearing sulfides over a broad range of sulfur fugacity because the Ru sulfidation curve is located several log units below that of Os-Ir.

CONCLUSION

The present-day sulfide assemblages in NWA 2737 are postshock assemblages, postdating S devolatilization and reduction of Fe sulfides into troilite and alloys, either Fe-Ni or Os-Ir-rich. The S devolatilization event also eliminated Martian Ca-sulfates.

It is widely assumed that shock impacts may have demagnetized the Martian crust in area of impact craters (Rochette et al. 2005; Louzada et al. 2011). Pre-impact field can be erased via shock hardening of the pyrrhotite (accumulation of defects), or heating of monoclinic pyrrhotite, an important ferromagnetic mineral and a significant contributor to remnant magnetic field in the upper (30 km) Martian crust above its Curie temperature (320 °C). The mineralogy in NWA 2737 suggests

alternative mechanisms to a simple heating processes, in showing that shock-induced S devolatilization can generate a low-temperature 2C troilite structure that is paramagnetic (e.g., Bennet and Graham 1981; Dekkers 1989). Local excursion of pyrrhotite compositions toward troilitic endmembers were previously reported in Nakhla (Bunch and Reid 1975), Governador Valadares and Lafayette (Bunch and Reid 1975), and Chassigny (Floran et al. 1978). These troilite-like compositions may be signs of localized shock-induced S losses.

Pyrrhotite readily oxidizes in supergene conditions of terrestrial atmospheric weathering (e.g., Mikhlin et al. 2002; Lorand et al. 2005). The astonishingly fresh nature of NWA 2737 sulfides can result from the short exposure of this chassignite to surface weathering (as suggested by low Ba and Sr contents; Beck et al. 2006) and/or an effect of the vacancy-free recrystallized stoichiometric troilite composition. Janzen et al. (2000) determined by experiments that low starting deficiency of iron in pyrrhotite correlates with the minimum oxygen concentration in the neutral alteration layer and the slowest alteration rates.

Editorial Handling—Dr. Randy Korotev

REFERENCES

Alard O., Griffin W. L., Lorand J.-P., Pearson N., and O'Reilly S. Y. 2000. Non-chondritic HSE patterns in mantle sulfides. *Nature* 407:891–894.

Bai W., Robinson P. T., Fang Q., Yang J., Yan B., Zhang Z., Hu X. H., Zhou M. F., and Malpas J. 2000. The PGE and base-metal alloys in the podiform chromitites of the Luobusa opholite, Southern Tibet. *Canadian Mineralogist* 38:585–598.

Barin I. 1995. *Thermochemical data of pure substances*. Weinheim: VCH. 1885 p.

Barnes S.-J., van Achterbergh E., Makovicky E., and Li C. 2001. Proton microprobe results for the partitioning of platinum-group elements between monosulfide solid solution and sulphide liquid. *South African Journal of Geology* 104:275–286.

Barton P. B. 1970. Sulfide petrology. *Mineralogical Society of America Special Paper* 3:187–198.

Beck P., Barrat J. A., Gillet P., Wadhwa M., Franchi I. A., Greenwood R. C., Bohn M., Cotten J., van de Moortèle B., and Reynard B. 2006. Petrography and geochemistry of the chassignite Northwest Africa 2737 (NWA 2737). *Geochimica et Cosmochimica Acta* 70:2127–2139.

Bennet C. E. G. and Graham J. 1981. New observations on natural pyrrhotites: Magnetic transition in hexagonal pyrrhotite. *American Mineralogist* 66:1254–1257.

Bird J. M. and Bassett W. A. 1980. Evidence of a deep mantle history in terrestrial osmium-iridium-ruthenium alloys. *Journal of Geophysical Research* 85:5461–5470.

Bläss U. W., Langenhorst F., and McCammon C. 2010. Microstructural investigations on strongly stained olivines of the chassignite NWA 2737 and implications for its shock history. *Earth and Planetary Science Letters* 300:255–263.

Bockrath C., Ballhaus C., and Holzheid A. 2004. Stabilities of Laurite RuS2 and monosulfide liquid solutions at magmatic temperatures. In *Highly siderophile elements and igneous processes*, edited by Reisberg L., Lorand J.-P., Alard O., and Ohnenstetter M. *Chemical Geology* 208:247–264.

Bodgard D. D. and Garrison D. H. 2008. ^{39}Ar–^{40}Ar age and thermal history of Martian dunite NWA 2737. *Earth and Planetary Science Letters* 273:386–392.

Brearley A. J. and Jones R. H. 1997. Chondritic meteorites. In *Planetary materials*, edited by Papike J. J. Reviews in Mineralogy, vol. 36. Washington, D.C.: Mineralogical Society of America. pp. 3-001–3-398.

Brenan J. M., Cherniak D. J., and Rose L. A. 2000. Diffusion of osmium in pyrrhotite and pyrite: Implications for closure of the Re-Os isotopic system. *Earth and Planetary Science Letters* 180:399–413.

Bullanova G. P., Griffin W. L., Ryan C. G., Shestakova Ye O., and Barnes S. J. 1996. Trace elements in sulfide inclusion from Yakutian diamonds. *Contributions to Mineralogy and Petrology* 124:111–125.

Bunch T. E and Reid A. M. 1975. The nakhlites. I. Petrography and mineral chemistry. *Meteoritics* 10:303–315.

Burgess R., Wright I. P., and Pillinger C. T. 1989. Distribution of sulphides and oxidized sulphur components in SNC meteorites. *Earth and Planetary Science Letters* 93:314–320.

Carpenter R. H. and Bailey A. 1973. Application of Ro and Ar measurements to the study of pyrrhotite and troilite. *American Mineralogist* 58:440–443.

Chevrier V., Lorand J.-P., and Sautter V. 2011. Sulfide petrology of four nakhlites (NWA 817, NWA 998, Nakhla, Governador Valadares). *Meteoritics & Planetary Science* 46:769–784.

Clarke R. Y. and Scott E. R. D. 1980. Tetrataenite-ordered FeNi, a new mineral in meteorites. *American Mineralogist* 65:624–630.

Dekkers M. J. 1989. Magnetic properties of natural pyrrhotite. Part II: High and low-temperature behavior of Jrs and TRM as a function of grain size. *Physics of the Earth and Planetary Interiors* 57:266–283.

Delaney J. S. and Dyar M. D. 2001. Magmatic magnetite in Martian meteorite melt inclusions from Chassigny (abstract). *Meteoritics* 36:A48.

Eggler D. H. and Lorand J.-P. 1993. Mantle sulfide oxybarometry. *Geochimica et Cosmochimica Acta* 57:2213–2222.

Etschmann B., Pring A., Putnis A., Grguric B. A., and Studer A. 2004. A kinetic study of the exsolution of pentlandite (Ni,Fe)9S8 from the monosulfide solid solution (Fe,Ni)S. *American Mineralogist* 89:39–50.

Ewers W. E. 1972. Nickel-iron exchange in pyrrhotite. *Proceedings of the Australasian Institute of Mining and Metallurgy* 241:10–25.

Farquhar J., Kim S. T., and Masterson A. 2007. Implications from sulfur isotopes of the Nakhla meteorite for the origin

of sulfate on Mars. *Earth and Planetary Science Letters* 264:1–8.

Fleet M. E. and Stone W. E. 1991. Partitioning of platinum-group elements in the Fe-Ni-S system and their fractionation in nature. *Geochimica et Cosmochimica Acta* 55:245–253.

Floran R. J., Printz M., Hlava P. F., Keil K., Nehru C. E., and Hinthorne J. R. 1978. The Chassigny meteorite: A cumulate dunite with hydrous amphibole-bearing melt inclusions. *Geochimica et Cosmochimica Acta* 42:1213–1229.

Greenwood J. P., Mojzsis S. J., and Coath C. D. 2000. Sulfur isotopic compositions of individual sulfides in Martian meteorites ALH84001 and Nakhla: Implications for crust-regolith exchange on Mars. *Earth and Planetary Science Letters* 184:23–35.

Ikeda Y., Yamamoto T., Kojima H., Imae N., Kong P., and Ebihara M. 1997. Yamato-791093, a metal-sulfide-enriched H-group chondritic meteorite transitional to primitive IIE irons with silicate inclusions. *Antarctic Meteorite Research* 10:335–353.

Janzen M. P., Nicholson R. V., and Scharer J. M. 2000. Pyrrhotite reaction kinetics: Reaction rates for oxidation by oxygen, ferric iron, and for nonoxidative dissolution. *Geochimica et Cosmochimica Acta* 64:1511–1522.

Jones J. H., Neal C. R., and Ely J. C. 2003. Signatures of the highly siderophile elements in the SNC meteorites and Mars, a review and petrologic synthese. *Chemical Geology* 196:57–76.

Joreau P., French B. M., and Doukhan J.-C. 1996. A TEM investigation of shock metamorphism in quartz from the Sudbury impact structure (Canada). *Earth and Planetary Science Letters* 138:137–143.

Karup-Møller S. and Makovicky E. 1995. The phase system Fe–Ni– S at 725 °C. *Neues Jahrbuch fur Mineralogie, Monatshefte* 1:1–10.

Kimura M. and Ikeda Y. 1992. Mineralogy and petrology of an unusual Belgica-7904 carbonaceous chondrite: Genetic relationships between the components. *Proceedings of the NIPR Symposium on Antarctic Meteorites* 5:72–117.

Kimura M., Grossman J. N., and Weisberg M. K. 2008. Fe-Ni metal in primitive chondrites: Indicators of classification and metamorphic conditions for ordinary and CO chondrites. *Meteoritics & Planetary Science* 43:1161–1177.

Kimura M., Grossman J. N., and Weisberg M. K. 2011. Fe-Ni metal and sulfide minerals in CM chondrites: An indicator for thermal history. *Meteoritics & Planetary Science* 46:431–442.

Knauth L. P., Burt D. M., and Wohletz K. H. 2005. Impact origin of sediments at the opportunity landing site on Mars. *Nature* 438:1123–1128.

Kullerud G., Yund R. A., and Moh G. H. 1969. Phase relations in the Cu-Fe-S, Cu-Ni-S and Fe-Ni-S systems. In *Magmatic ore deposits*, edited by Wilson H. D. B. Lancaster, Pennsylvania: Economic Geology Publishing Co. pp. 323–343.

Li C., Barnes S.-J., Makovicky E., Rose-Hansen J., and Makovicky M. 1996. Partitioning of nickel, copper, iridium, rhenium, platinum and palladium between monosulfide solid solution and sulfide liquid: Effects of composition and temperature. *Geochimica et Cosmochimica Acta* 60:1231–1238.

Lorand J.-P. 1985. The behaviour of the upper mantle sulfide component during the incipient serpentinization of "alpine-type" peridotites as exemplified by the Beni Bousera (Northern Morocco) and Ronda (Southern Spain)

ultramafic bodies. *Tschemarks Mineralogische und Petrographische Mitteilungen* 34:183–209.

Lorand J.-P. 1988. The Cu-Fe-Ni sulfide assemblages of tectonic peridotites from the Maqsad district, Sumail ophiolite, Southern Oman: Implications for the origin of the sulfide component in the oceanic upper-mantle. In *The ophiolites of Oman*, edited by Boudier F. and Nicolas A. *Tectonophysics* 151:57–74.

Lorand J.-P. and Alard O. 2001. Geochemistry of platinum-group elements in the subcontinental lithospheric mantle; in-situ and whole-rock analyses of some spinel peridotite xenoliths, Massif Central, France. *Geochimica et Cosmochimica Acta* 65:2789–2806.

Lorand J.-P., Chevrier V., and Sautter V. 2005. Sulfide mineralogy and redox conditions in some Shergottites. *Meteoritics & Planetary Science Letters* 40:1257–1272.

Louzada K. L., Stewart S. T., Weiss B. P., Gattacceca J., Lillis R. J., and Halekas S. J. 2011. Impact demagnetization of the Martian crust: Current knowledge and future directions. *Earth and Planetary Science Letters* 305:257–269.

MacQueen K. G. 1979. Experimental heating and diffusion effects in the Fe-Ni-S ore from Redross, Western Australia. *Economic Geology* 74:140–148.

Malavergne V., Guyot F., Benzerara K., and Martinez I. 2001. Description of new shock-induced phases in the Shergotty, Zagami, Nakhla and Chassigny meteorites. *Meteoritics & Planetary Science* 36:1297–1305.

Mallmann G. and O'Neill H. St. C. 2009. The crystal/melt partitioning of V during mantle melting as a funtion of oxygen fugacity compared with some other elements (Al, P, Ca, Sc, Ti, Cr, Fe, Ga, Y, Zr and Nb). *Journal of Petrology* 50:1765–1794.

McSween H. Y., Jr. 2002. The rocks of Mars, from far and near. *Meteoritics & Planetary Science* 37:7–25.

McSween H. Y., Jr. and Treiman A. H. 1997. Martian meteorites. In *Planetary materials*, edited by Ribbe P. H. Reviews in Mineralogy, vol. 36. Washington, D.C.: Mineralogical Society of America. pp. 6-01–6-54.

Mikhlin Y. L., Kuklinskiy A. V., Pavlenko N. I., Varnek V. A., Asanov I. P., Okotrub A. V., Selyutin G. E., and Solovyev L. A. 2002. Spectroscopic and XRD studies of the air degradation of acid-reacted pyrrhotites. *Geochimica et Cosmochimica Acta* 66:4057–4067.

Misra K. C. and Fleet M. E. 1973. The chemical composition of synthetic and natural pentlandite assemblages. *Economic Geology* 68:519–538.

Murck B. W and Campbell I. H. 1986. The effects of T, fO_2 and melt composition on the behaviour of Cr in basic and ultrabasic melts. *Geochemica et Cosmochimica Acta* 50:1871–1883.

Nyquist E., Bogard D. D., Shih C. Y., Greshake A., Stöffler D., and Eugster O. 2001. Ages and geologic histories of Martian meteorites. In *Chronology and evolution of Mars*, edited by Kallenbach R., Geiss J. and Hartmann W. K. Dordrecht: Kluwer. pp. 105–164.

Pedersen A. K. 1979. Basaltic glass with high-temperature equilibrated immiscible sulphide bodies with native iron from Disko, central West Greenland. *Contributions to Mineralogy and Petrology* 69:397–407.

Peregoedova A., Barnes S.-J., and Baker D. R., 2004. The formation of Pt-Ir alloys and Cu-Pd-rich sulfide melts by partial desulfuration of Fe-Ni-Cu sulfides: Results of experiments and implications for natural systems. In *Highly siderophile elements and igneous processes*, edited by

Reisberg L., Lorand J.-P., Alard O., and Ohnenstetter M. *Chemical Geology* 208:247–264.

Pieters C. M., Klima R. L., Hiroi T., Dyar M. D., Lane M. D., Treiman A. H., Noble S. K., Sunshine J. M., and Bishop J. L. 2008. Martian dunite NWA 2737: Integrated spectroscopic analyses of brown olivine. *Journal of Geophysical Research* 113:E06004. doi: 10.1029/2007/JE002939.

Rochette P., Lorand J.-P., Fillion G., and Sautter V. 2001. Pyrrhotite and the remanent magnetization of SNC meteorites: A changing perpective on Martian magnetism. *Earth and Planetary Science Letters* 190:1–12.

Rochette P., Gattacceca J., Chevrier V., Hohmann V., Lorand J.-P., Funaki M., and Hochleitner R. 2005. Matching martian magnetic anomalies and meteorite magnetic properties. *Meteoritics & Planetary Science* 40:529–540.

Roedder P. and Reynolds I. 1991. Crystallization of chromite and chromium solubility in basaltic melts. *Journal of Petrology* 32:909–934.

Stöffler D., Ostertag R., Jammes C., Pfanschmidt G., Gupta P. R. S., Simon S. B., Papike J. J., and Beauchamp R. H. 1986. Shock metamorphism and petrography of the Shergotty achondrite. *Geochimica et Cosmochimica Acta* 50:889–903.

Stöffler D., Keil K., and Scott E. R. D. 1991. Shock metamorphism of ordinary chondrites. *Geochimica et Cosmochimica Acta* 55:3845–3867.

Toulmin P. and Barton P. B. 1964. A thermodynamic study of pyrite and pyrrhotite. *Geochimica et Cosmochimica Acta* 28:641–671.

Treiman A. H., Gleason J. D., and Bogard D. D. 2000. The SNC meteorites are from Mars. *Planetary and Space Science* 48:1213–1230.

Treiman A. H., Dyar M. D., McCanta M., Noble S. K., and Pieters C. M. 2007. Martian dunite NWA 2737: Petrographic constraints on geological history, shock events, and olivine color. *Journal of Geophysical Research* 112: E04002. doi:10.1029/2006JE002777.

Uehara M., Gattacceca J., Leroux H., Jacob D., and van der Beek C. D. 2011. Magnetic microstructures of metal grains in equilibrated ordinary chondrites and implications for paleomagnetism of meteorites. *Earth and Planetary Science Letters* 306:241–252.

Van de Moortèle B., Reynard B., Rochette P., Jackson M., Beck P., Gillet P., McMillan P. F., and McCammon C. A. 2007. Shock-induced metallic iron nanoparticles in olivine-rich Martian meteorites. *Earth and Planetary Science Letters* 262:37–49.

Vaughan D. J. and Craig J. R. 1978. *Mineral chemistry of metal sulfides*. Cambridge: Cambridge University Press. 493 p.

Wenworth S. J., and Goodings J. L. 1994. Carbonates and sulfates in Chassigny meteorites; further evidence for aqueous alteration on the SNC parent body. *Meteoritics* 29:860–863.

Yang C. W., Williams D. B., and Goldstein J. I. 1997. Low-temperature phase decomposition in metal from iron, stony-iron, and stony meteorites. *Geochimica et Cosmochimica Acta* 61:2943–2956.